Memoirs of the Scientific Sections of the Romanian Academy
Tome XLIII, 2020

CHEMISTRY

POLYROTAXANES CONSTRUCTED FROM CUCURBIT[7]URIL AND Π-CONJUGATED POLYMERS

AURICA FARCAS

"Petru Poni" Institute of Macromolecular Chemistry, 700487 Iasi, Romania
afarcas@icmpp.ro

This study summarizes our recent endeavors, related to the design, synthesis, and photophysical characteristics of polythiophenes and polyfluorenes homo- or copolymers, and poly(3,4-ethylenedioxythiophene) encapsulated into cucurbit[7]uril (CB7) cavities involving different synthetic strategies. For the sake of comparison, the photophysical properties of these polyrotaxanes were compared to those of their nonthreaded homologs. CB7-based conjugated polyrotaxanes exhibit advantageous photophysical and transport properties, which makes them suitable in optoelectronic applications.

Keywords:Host-guestsystem, cucurbit[7]uril, semiconductors, macrocycles, HOMO-LUMO, fluorescence, electronic devices.

1. INTRODUCTION

Over the past decades, conjugated polymers (CPs) have been actively investigated as an alternative to conventional inorganic materials, due to their low cost and easy processability as next generation organic electronic devices [1]. In order to replace inorganic semiconductors, CPs need to render high photoluminescence (PL) and fluorescence quantum yield (Φ_{PL}) in solid state, as well as a better balance between the injection and transport of electrons and holes [2]. Although tremendous effort has been devoted to tune CPs's photophysical and charge-transport properties through molecular design, undesirable intermolecular interactions, which affect Φ_{PL}, electrical transport and environmental stability, considerably limit their applications [3]. The past decade has witnessed remarkable innovations and progress in polymer science, including supramolecular science as complementary field, which offers great opportunity for new concepts and new materials. The construction of mechanically interlocked molecules, such as conjugated polyrotaxanes (CPRs), has attracted considerable attention due to their architectures and topologies, but mostly because they provide an efficient strategy to achieve an "insulation" of individual molecular wires (IMWs) [4–7]. The synthesis of such supramolecular compounds is based on the molecular recognition principle and is

the result of the cooperation of various non-covalent interactions. The presence of macrocycles suppresses intermolecular interactions and effectively inhibits interchain interactions by increasing separation distances between the CPs backbones. Despite these improvements, threading of CPs backbones into macrocycles leads to an increased solubility in common organic solvents, environmental stability and resistance to quenching from solvent or impurities. These architectures preserve the semiconducting properties of conjugated backbones and keep the conjugated chains at a minimum separation distance, imposed by the thickness of the macrocycle walls. Furthermore, previously photophysical and electronic studies of such supramolecular compounds showed that even incomplete shielding preserved the photophysics of the isolated conjugated backbones, without affecting charged transport properties [4–11]. The strategy applied for the synthesis of such supramolecular compounds is encapsulation of π-conjugated monomers (guests) with suitable macrocycles (hosts) by simply threading the guest backbones through host cavities without any covalent bonds between them, followed by polymerization, pseudopolyrotaxane (PSs) systems thus resulting. To avoid dethreading of the macrocycles, bulky stoppers are covalently attached at both ends of the PSs and, finally, polyrotaxane (PRs) are obtained. Conjugated/ insulated monomers/ polymers (guests) that satisfy the requisite steric and charge characteristics can be encapsulated by different host macrocycles. As host molecules, native cyclodextrins (CDs) and their partially or permodified derivatives are by far the most intensively investigated host molecules for the synthesis of such supramolecular architectures [8–11]. Lower propensity to aggregate formations of chemically-permodified CDs, such as 2,3,6-tri-O-methyl CD (TMe-CD), 2,3,6-tri-O-trimethylsilyl CD (TMS-CD), better solubility in water or common organic solvents, easier processability and transparency nature of the solid films represent noticeable advantages with regard to optoelectronic applications. Most recently, cucurbit[7]uril (CB7) has aroused a lot of interest in our research group, as it is considered also a very promising host for the synthesis of such organized systems. Its chemical constitution, a hydrophobic cavity and two identical and highly polarizable carbonyl portals of the cavity, as well as its high binding affinity toward neutral and cationic guests has made it a subject of interest [7,12–14].

The aim of the present review is to provide the reader an overview on the approaches that have been employed to synthesize three types of CB7-based conjugated PRs, and to show that encapsulation into CB7 cavities could effectively improve CPs's water solubility, optical and morphological characteristics, which are advantageous traits for their applications in optoelectronic. This study summarizes our recent endeavors, related to the design, synthesis, and properties of polythiophenes (PTs), polyfluorenes (PFs) homo- or copolymers and poly(3,4-ethylenedioxythiophene) (PEDOT) encapsulated into CB7, involving two synthetic strategies. For the sake of comparison, the photophysical properties of these new self-organized systems were compared to those of their non-threaded homologs.

2. CONJUGATED POLYROTAXANES

2.1. POLY[2,7-(9,9-DIOCTYLFLUORENE)-*ALT*-(5,5′-BITHIOPHENE/CB7) ROTAXANE COPOLYMER

The alternating copolymer containing fluorene and bithiophene units has proved to be one of the most promising conjugated polymers, due to its good hole transporting properties and thermotropic liquid crystallinity, which allows a better packing of polymer chains *via* self-assembly [15]. Although these properties may be generally acceptable for generating the active layers in electronic devices, this copolymer has poor stability against oxidation and easily undergoes photo-oxidation [5]. To prevent such undesired oxidation tendency, encapsulation of conjugated monomers into macrocyclic host molecules, followed by polymerization, has been employed as an alternative approach to achieve supramolecular PRs structures. By Suzuki cross-coupling of a 1/1 molar ratio of 5,5'-dibromo-2,2'-bithiophene (BT) encapsulated into CB7 cavities with 9,9-dioctylfluorene-2,7-diboronic acid bis(1,3-propanediol) ester as difunctional bulky stoppers PF-BT·CB7 PRs, as well as their non-rotaxane counterpart (PF-BT) have been synthesized and photophysically characterized [7]. The chemical structures of these compounds are plotted in Figure 1.

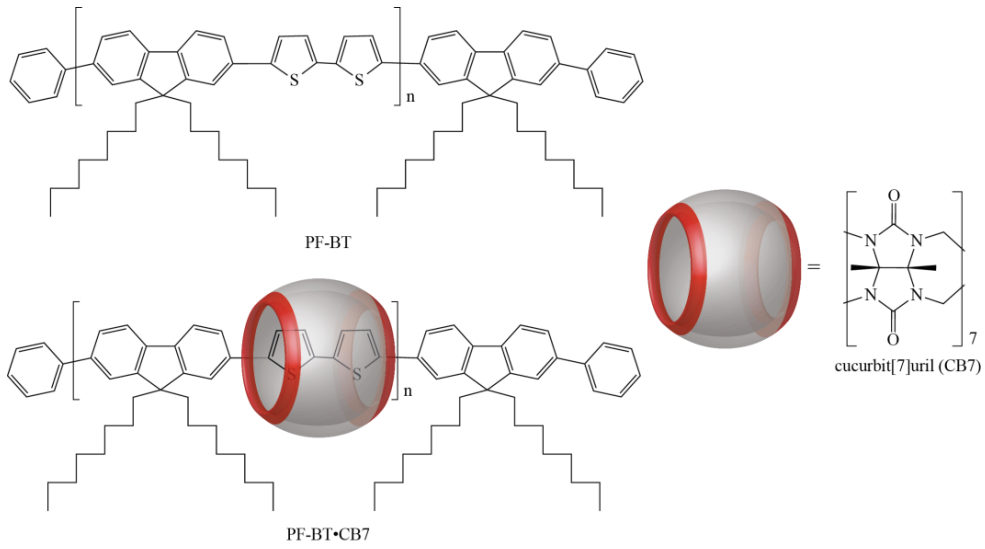

Fig. 1. Chemical structures of PF-BT and PF-BT·CB7 PRs.

The Suzuki cross-coupling reactions were performed with 1/1 CB7/BT encapsulation, yet the resulting PF-BT·CB7 PR contains only 28% coverage (quantified by ^{1}H NMR) [7]. The lower rotaxane content can be attributed to the adverse effect of high temperature (necessary for Suzuki coupling) on the stability

of BT·CB7 inclusion complexes (ICs). Worth mentioning is that PF-BT·CB7 PRs exhibited good solubility in water (about 10% by weight after vortex stirring at 60°C for 30 min and about 18% in THF/H_2O 1/1 v/v mixture). The thermal properties of these compounds were evaluated by TGA and DSC analysis. TGA data revealed that both compounds were stable up to 300°C. The non-rotaxane PF-BT exhibits T_g of about 75°C. The higher value of T_g for PF-BT·CB7 PRs proves the increase in rigidity of the copolymer structures when the BT backbone is threaded through the macrocyclic CB7 cavity. Rotaxane formation results in improvements of thermal stability, solubility in common organic solvents, as well as in better film forming ability combined with a high transparency. The effect of CB7 on the optical properties of PF-BT·CB7 was also investigated and compared with that of the non-rotaxane PF-BT counterpart. As expected, PF-BT absorbs beyond 510 nm, with a maximum at 450 nm. Inclusion of BT inside the CB7 cavity caused a clear hypsochromic shift of 60 nm (390 nm), along with a prominent shoulder at ~ 430 nm and broadening in the absorption spectra. The PL properties in solution have also been investigated. PF-BT has an emission spectrum with two peaks at ~ 498 and 527 nm, and a weak shoulder at ~ 560 nm. These peaks are slightly blue-shifted (494 and 521 nm), while the shoulder becomes less intense (~ 560 nm) in PF-BT·CB7, and Φ_{PL} decreases from 0.5 to 0.4 in the PF-BT·CB7. Therefore, it is very likely that encapsulation increases the charge transfer character of the excited state of PF-BT, which is also reflected in increased stokes shift - from 77 to 91 nm. The fluorescence lifetime decay traces (τ_f) of compounds were monoexponential, and the very low polarizability of PF-BT inside the CB7 increased its lifetime from 630 to 665 ns. Changes in the optical properties of the PF-BT copolymer could be attributed to a relatively strong interaction between CB7 and the conjugated cores, as testified by the monomolecular exponential decay of PL. The redox properties were also investigated by cyclic voltammetry (CV). PF-BT·CB7 exhibits typical semiconducting properties, that is, an insulating behavior (i=0) over a wide range of potential between the *n*- and *p*-doping processes at both negative and positive potentials, respectively. The first CV scan of PF-BT·CB7 is different from the subsequent ones, a behavior attributed to the evolution of the electrochemical interface between polymer and solution, as the electrochemical response is stable at the second CV scan. During the first CV scan, the *n*- or *p*-doping is accompanied by insertion or removal of the counterions and solvent molecules into or from the polymer film, which involves a gradual opening of the morphology of the studied sample with an evolution of the CV shape upon repetitive scans. This behavior has been previously observed for other conjugated PRs [16]. During the *n*-doping process, PF-BT·CB7 polyrotaxane is reduced to a lower potential (-1.67 V), compared to the reference PF-BT. This behavior is presumably induced by the stronger electron density of the carbonyl rim of the CB7 macrocycle, acting on the π-PF-BT backbones. The electron-donating character of the carbonyl rim of the CB7 macrocycle is also slightly reflected in the *p*-doping process, as the onset oxidative potential occurs with a negative shift of 120–130 mV at 1.05 V.

Surface topography of compounds was investigated by atomic force microscopy (AFM) on spin-coated thin films, the AFM images clearly indicating a rod-like structure for all copolymer samples. Threading of CB7 onto PF-BT chains leads to less conformational flexibility of its macromolecular chains and to a higher tendency to organize into linear ribbons (Fig. 2). The observed variations in surface topography, compared to reference PF-BT, provide further evidence of the change in PRs packing geometries induced by the nature of the macrocycle used in the synthesis of such conjugated PRs. It should be pointed out that AFM images of PF-BT covered by TMe-βCD or TMS-βCD reveals the tendency of PF-BT to self-organize on fibers in solid state [8].

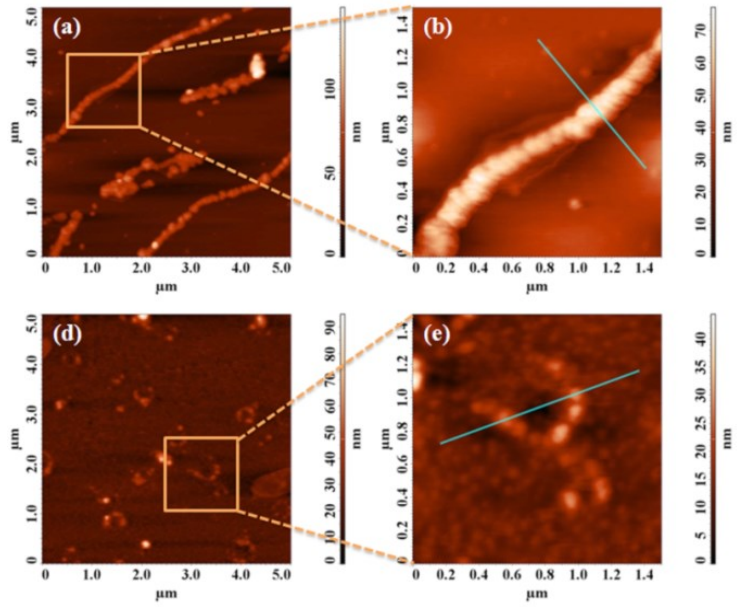

Fig. 2. 2D AFM topography images of spin-coated poly[2,7-(9,9-dioctylfluorene)-alt-(5,5`-bithiophene/ CB7)] film on mica substrate (a,b) and its non-rotaxane counterpart (d,e).

To gain further insight into the effect of CB7 encapsulations, advancing contact angles (θ) values of water and diiodomethane, as well as surface free-energies (γ_S) with their dispersive (γ_S^d) and polar (γ_S^p) components have been obtained for spin-coated copolymer films, the results obtained being summarized in Table 1. The lower value of θ in water for PF-BT·CB7 compared with that of PF-BT (reference), clearly indicates the decreases in the hydrophobicity of PF-BT surface. In addition, the significant increase in the value of the polar component (γ_S^p) for polyrotaxane PF-BT·CB7 is the consequence of the contribution of the negatively charged carbonyl portals of CB7 to the total surface free-energy of the system.

Table 1

Advancing contact angle of water and diiodometane measured on spin-coated film of PF-BT and PF-BT·CB7 compounds

Samples	θ (°)[a]	θ (°)[b]	γ_S (mN·m^{-1})[c]	γ_S^d (mN·m^{-1})[d]	γ_S^p (mN·m^{-1})[e]
PF-BT·CB7[f]	52.5 ± 2.7	64.0 ± 1.0	51.2	29.5	21.7
PF-BT[g]	69.6 ± 1.2	42.4 ± 1.1	40.8	29.9	10.9

[a,b] the advancing contact angle of water and diidomethane, respectively; [c] total surface free energy; [d] dispersion forces; [e] polar components; [f] data taken over from ref. [7]; [g] data taken over from ref. [8]

The obtained results suggest that CB7 encapsulation may be of practical utility in the development of these supramolecular assemblies, which can open a wide range of opportunities in the area of nanotechnology, *e.g.* as components of molecular necklaces.

2.2. CB7-BASED FLUORENE POLYROTAXANES

Polyfluorenes (PFs) have been intensively studied as emitting materials, owing to their pure blue emission [17,18]. Major drawbacks for PFs are their high ionization potential associated with low PL efficiency, rather large band gap and facile photochemical degradation [19,20]. Different strategies have been employed to reduce these undesirable effects, *e.g.*, the synthesis of copolymers or block copolymers [21,22], cross-conjugated polymers [23], introduction of donor and acceptor moieties [24,25], nanochannels [26] or wrapping of chromophores with amylose [27]. Among them, the construction of PRs architectures represents an attractive approach to achieve control over molecular rigidity, prevention of aggregation, improved PL, and surface-morphological characteristics of the resulting conjugated polyrotaxanes. The fluorene-based polyrotaxanes containing native [28-30], permethylated, [31], and persilylated [32] CDs reported by us showed significant improvements in solubility, surface characteristics, and other photophysical characteristics. Motivated by CB7's exceptional recognition properties in aqueous media, we used this macrocycle to form stable host-guest complexes with 2,7-dibromofluorene (**1**), a key precursor in the synthesis of new PF/CB7PRs [12]. It should be pointed out that encapsulation of **1** into CB7 cavities has been used to protect the 9 position of the fluorene moiety against oxidative degradation. The Suzuki cross-coupling reaction of **1**, either in its non-complexed state or as an inclusion complex with CB7 (**1·CB7**) with 9,9-dioctylfluorene-2,7-diboronic acid bis(1,3-propanediol) ester (**2**), yielded the neat **3** and its corresponding **3·CB7** fluorene polyrotaxane, respectively (Scheme 1). In this approach, a small excess of **2** was added at the end of polymerization to introduce ester groups at both polymer chain ends and, finally, bromobenzene as a monofunctional end-capping reagent to react the boronic ester end groups.

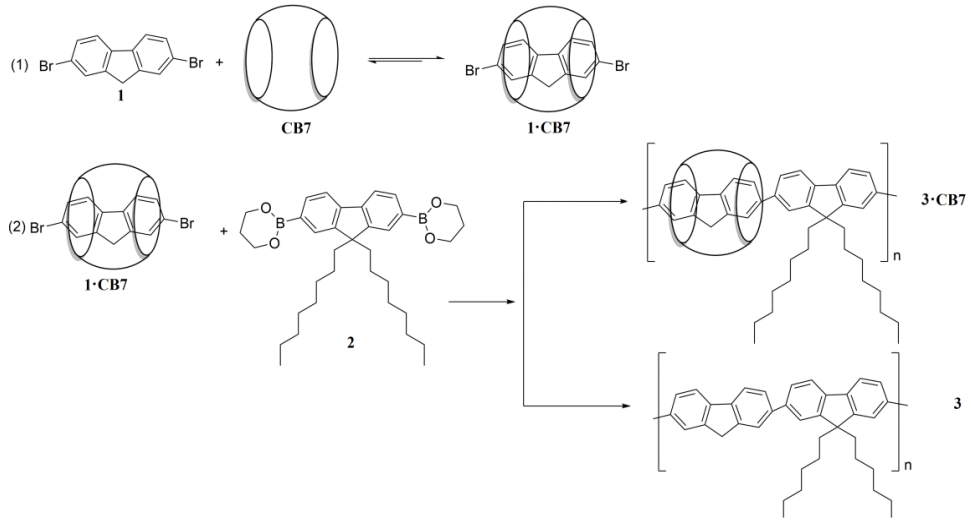

Scheme 1. Synthesis of **3·CB7** polyrotaxane and its non-rotaxane **3** counterpart.

Binding of monomer **1** with CB7, investigated by UV-vis absorption in water, was found to be 9.5 × 10^3 M^{-1} (Fig. 3). This value indicates that the studied aromatic guest **1** shows a stronger binding to CB7 than other macrocycles, being attributed to more favorable hydrophobic interactions. The thermal properties of **3·CB7** and **3** copolymers were investigated by TGA and DSC. The TGA curves revealed that both copolymers were stable up to ca. 300°C. DSC measurement of the neat copolymer **3** showed a distinct glass transition temperature (T_g) at 89°C, while the T_g value of **3·CB7** increased to 113°C [12]. The increased T_g of **3·CB7** supports the encapsulation of monomer **1** into the CB7 cavity, which confers more rigidity onto the PFs backbones. The increased T_g values are highly desirable for the use of PFs as emissive materials in light-emitting devices.

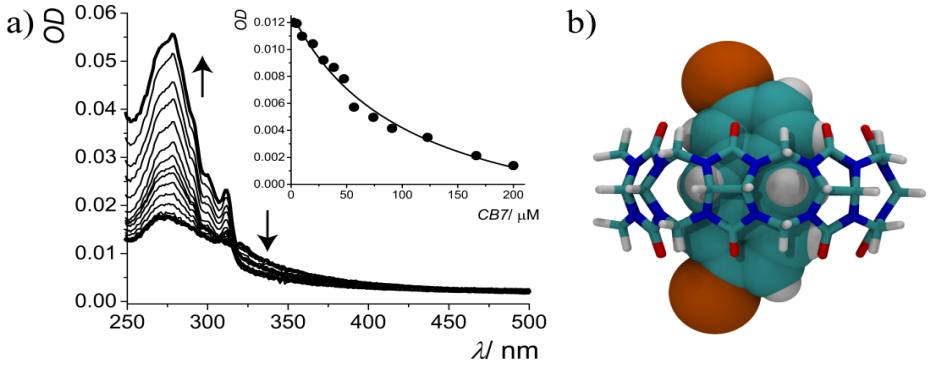

Fig. 3. a) Changes in the UV-vis absorption spectrum of a 2-μM solution of **1** upon increasing the CB7 concentration in water; Inset: the nonlinear fitting based on the UV-vis absorption change, assuming a 1:1 binding model. b) DFT-optimized structure of the **1·CB7** complex.

The effect of CB7 encapsulation on the optical properties was also investigated by UV-vis and PL measurements in a DMSO solution. The neat copolymer **3** showed a featureless band at 375 nm, while **3·CB7** exhibited a hypsochromic shift by 11 nm, which can be attributed to the reduction of intermolecular interactions and/ or to a variation of polarity, when the PFs core is complexed inside the CB7 cavity [33]. Emission of the neat copolymer **3** showed three vibronic components at 416, 440 and 473 nm. Surprisingly, **3·CB7** polyrotaxane exhibited a second emission band in the 500–600 nm regions, presumably due to aggregate or excimer emission [34]. Such interactions would be expected to display significantly longer lifetimes (τ_F) and non-monoexponential PL decay. The deviations from monoexponential decays are known for the non-homogeneous microenvironmental distributions of chromophores. However, we found out that τ_F for **3** and **3·CB7** in DMSO solutions followed a single exponential kinetics, with τ_F values of 0.6 and 0.7 ns, respectively. The origin of the long-wavelength emission can therefore not be further scrutinized for now. The redox properties *i.e*., the oxidation ($E_{p,onset}$) and reduction ($E_{n,onset}$) potentials were studied by CV. From the $E_{p,onset}$ and $E_{n,onset}$ values, the HOMO, LUMO and the electrochemical band gap (ΔE_g), as well the HOMO/LUMO positions in an energetic diagram were calculated. The electrochemical results suggest that the investigated **3** and **3·CB7** compounds should exhibit favorable semi-conducting properties (Fig. 4, left). During the *n*-doping process, electron affinity is reduced from −2.28 V for the neat copolymer **3** to −2.49 V for the polyrotaxane **3·CB7**, while the ΔE_g values shifted from 3.56 eV for **3** to 3.39 eV for **3·CB7**. These results suggest that CB7 imposes a more restricted environment onto the encapsulated redox-active fluorene chromophore. Comparison of the HOMO/LUMO energy levels of **3·CB7** polyrotaxane and the corresponding non-rotaxane **3** with the electronic potentials of the anodic indium tin oxide (ITO) glass substrate (−4.75 eV) and cathodic aluminum (−2.2 eV) [35] reveals that the required energy level criteria for the fabrication of organic light-emitting diodes (OLEDs) are nicely met (Fig. 4, right).

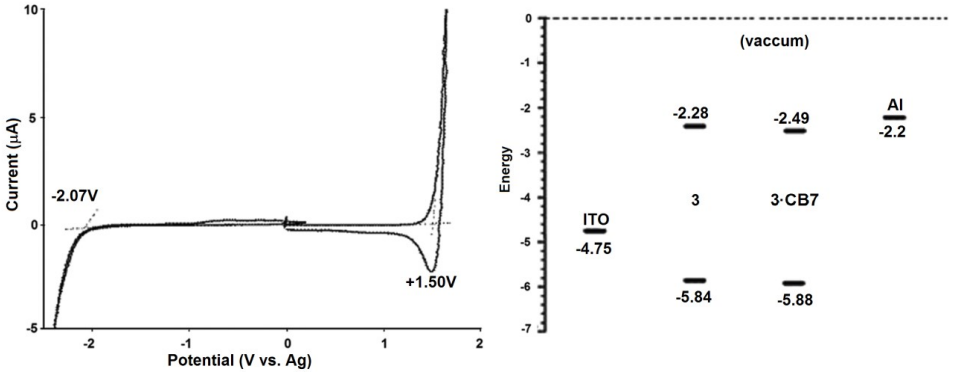

Fig. 4. CV of **3·CB7** in 0.1 M tetrabutylammonium perchlorate (TBAClO4)/ ACN solution at a scan rate of 20 mV·s−1 (left) and HOMO/ LUMO energy levels relative to the work functions of ITO (anode) and Al (cathode) (right).

Also investigated was the modification of the polymer structure by advancing contact angle measurements on **3** and **3·CB7** spin-coating films [12]. Advancing contact angles (θ_a) values of water and diiodomethane and surface free-energies (γ_s) with their dispersive (γ_s^d) and polar (γ_s^p) components were measured on spin-coated films of **3** and **3·CB7** copolymers, the results being summarized in Table 2. The spin-coated film of the neat **3** displayed a strong hydrophobicity, evidenced by a θ_a value close to 147° in water, as a result of the presence of the long hydrocarbon chains from monomer **2**. A significant decrease in hydrophobicity was observed for the spin-coated film of **3·CB7** ($\theta_a \sim 85°$), which is in good agreement with the incorporation of the CB7 macrocycle as a hydrophilic component. Interestingly, with diiodomethane as wetting agent, a higher θ_a value is obtained for **3·CB7** polyrotaxane (Table 2). The result clearly reveals drastic changes in the wettability properties, due to CB7 encapsulation.

Table 2

Advancing contact angles of water and diiodomethane and surface free-energies (γ_s) with their dispersive (γ_s^d) and polar (γ_s^p) components, in mN m^{-1}, obtained for spin-coated films made from **3** and **3·CB7** copolymers

Sample	θ_a(°)[a]		(γ_s)[b]	(γ_s^d)[c]	(γ_s^p)[d]	(γ_s^p/γ_s)[e]
	H_2O	CH_2I_2	(mN m^{-1})	(mN m^{-1})	(mN m^{-1})	(%)
3	147.0 ± 2.4	41.5 ± 1.1	3.8	3.6	0.2	5.3
3·CB7	84.8 ± 2.3	53.8 ± 1.4	28.3	22.1	6.2	21.9

[a] Advancing contact angle. [b] Total surface free energy. [c] Dispersion forces. [d] Polar components. [e] Percentage of polar component

Close inspection of the wetting results suggests that the dispersive component dominates for both **3** and **3·CB7** samples [12]. Taking into account that the morphology and microstructure are crucial features for device performance, the surface morphology, as well as the texture parameters of **3** and **3·CB7** thin films were further investigated by AFM. From an overall morphological point of view, the **3·CB7** film is more promising, due to its more uniform and smoother surface, compared to those obtained from the neat **3**. Even more, it is our special interest to explore the effect of CB7 encapsulations towards native CDs, as an alternative approach to bring some benefits on the photophysical properties of PFs, to which particular attention is paid to generating the active layer in organic electronic devices.

3.3. CB7- THREADED POLY(3,4-ETHYLENEDIOXYTHIOPHENE) (PEDOT)

Among the CPs, PEDOT, as a high electrical conducting polymer with low band-gap (E_g=1.4–1.6 eV) and good environmental stability, provided new opportunities for the development of innovative materials, opening new possibilities in science and technology [36]. PEDOT being insoluble in any

common solvent, “standard” solution characterization techniques (such as NMR spectroscopy) cannot be used, and features such as molecular weight remain often unrevealed. Recently, PEDOT-PSs and PRs having TMe-βCD as host molecules were reported by us, providing an efficient alternative to adjusting PEDOT solubility and processability, which allowed their use as an additive/ dopant free hole conductor in hybrid perovskite solar cells (PSCs) [37]. The use of CB7 for the synthesis of CB7-based PEDOT-PSs and PEDOT-PRs seems also very attractive, and should provide an unexpected opportunity in the creation of new supramolecular architectures with improved photophysical and transport properties. The synthetic strategy for the construction of these supramolecular compounds, as a first step in threading of 3,4-ethylenedioxythiophene (EDOT) into the CB7 cavity through host-guest complexation, results in the formation of EDOT·CB7 ICs. This architecture represents the starting monomer for the subsequent polymerization process, a common strategy in the synthesis of polyrotaxanes. Next, oxidative polymerization in water with a five-fold excess of iron (III) chloride ($FeCl_3$) allows the synthesis of PEDOT-PSs and, subsequently, attachment of a bulky stopper (pyrene) to PEDOT-PRs [14]. The chemical structures of these supramolecular compounds are illustrated in Figure 5. The uncomplexed PEDOT was also synthesized by the coupling reaction of an aqueous EDOT dispersion with $FeCl_3$ and, finally, by the addition of pyrene as a stopper.

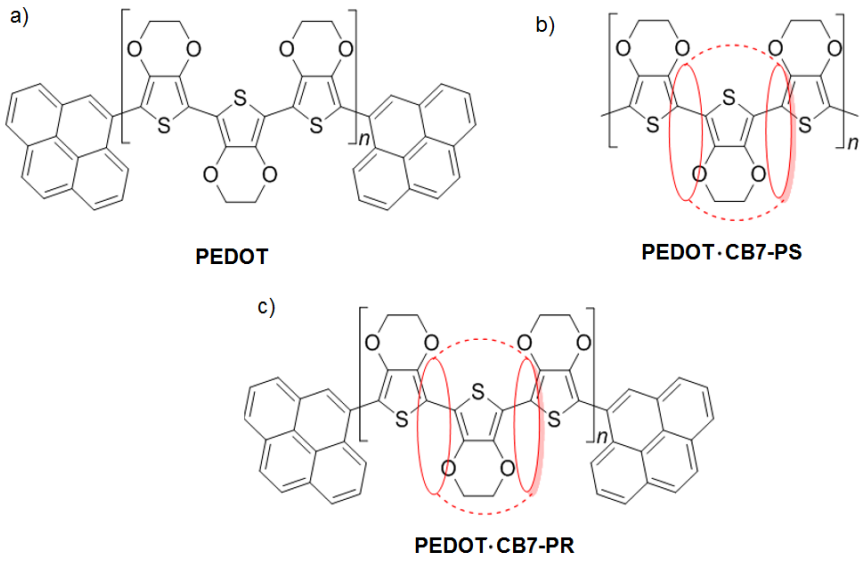

Fig. 5. Chemical structures of: a) PEDOT, b) PEDOT·CB7-PSs, c) and PEDOT·CB7-PRs.

The binding affinity (K_a) of EDOT to CB7 was evaluated by UV-Vis absorption in water. The obtained K_a value of 1.5 × 104 M^{-1} indicated a sizable binding of CB7 to EDOT as a neutral guest molecule, with a higher affinity than

CDs, attributed to the more favorable hydrophobic and dispersion interactions between EDOT and CB7. Additionally, density functional theory (DFT) calculations were carried out to further identify the synthesized compounds. Optimized ground-state geometries of a model PEDOT-trimer are shown in Figure 6. The optimized structure of the PEDOT-trimer showed that the EDOT units were oriented in an alternating direction.

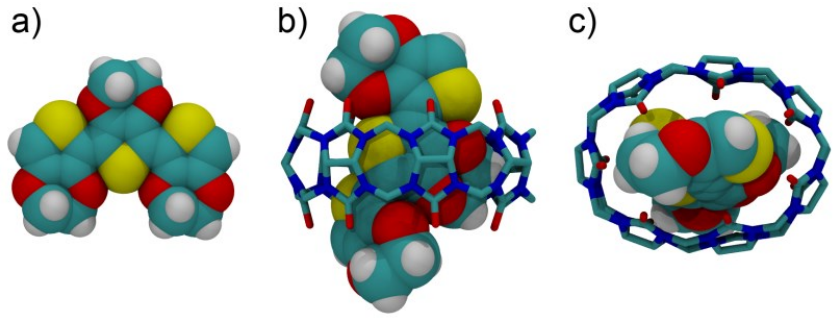

Fig. 6. DFT-optimized (wb97xd/3-21G*) structures of a PEDOT-trimer as a model: a) free; b) complexed with CB7 (side); c) complexed with CB7 (top).

The chemical structures of the synthesized compounds were verified by FT-IR and NMR spectroscopy. The ^{1}H NMR of the PEDOT·CB7 PRs soluble fraction in DMSO indicated a coverage ratio of about 35%, whereas the fraction soluble in water – around 60% [14]. TGA analysis indicated that PEDOT·CB7 PRs has a higher thermal stability than the corresponding PEDOT, which confirmed the beneficial effect of CB7 on the thermal stability of the PEDOT backbone. In addition, these materials are considered to be thermally stable up to 250^{o}C. Overall, no glass transitions or melting temperatures between 20 and 200°C were found for either compound. The absorption and emission spectra of the compounds were recorded in water and DMSO solutions. The absorption spectrum of the PEDOT·CB7-PRs fraction soluble in water is consistent with the spectrum of the neat PEDOT in DMSO. The bands at shorter and longer wavelengths correspond to the π-π^{*} transition and free charge carriers of the PEDOT polymer backbones, respectively. The fluorescence spectra revealed a clear bathochromic shift of PEDOT·CB7 PRs (~21 nm), relative to those of neat PEDOT and PEDOT·CB7 PSs. This can be attributed to a more planarized structure of PEDOT in the PRs architectures whereas, in PSs, the CB7 units might partially dissociate from the polymer backbone, leading to a more folded conformation. Furthermore, spectra for the PSs architectures and the PEDOT reference suggested that the electronic transitions are not affected by CB7 complexation itself, while the macrocycle only influences the global backbone conformation. Also estimated was the fluorescence quantum yield (Φ_{PL}) in DMSO solution at 339 nm excitation wavelength of PEDOT and PEDOT·CB7-PRs. Improvement of Φ_{PL} (by a factor of 2) of

PEDOT·CB7 PRs compared with PEDOT can be assigned to the relocation of PEDOT backbone into the more hydrophobic macrocyclic environment, which decreases non-radiative decay pathways. In order to highlight the improvements of solubility, PEDOT·CB7 PRs films were prepared by drop casting on freshly cleaved mica substrates of the fraction soluble in water, DMSO and a water/ DMSO 1/1 v/v mixture. Due to the insolubility of PEDOT in water and in the water/ DMSO mixture, thin films were prepared by deposition of its DMSO dispersion. It should be noted that the surface morphology of PEDOT·CB7 PRs was influenced by the solvent. Thus, the part soluble in DMSO was homogenously distributed on the surface with individual grains, spherically shaped, with two diameters (187±16 and 100±15 nm). The presence of water induced agglomeration, so that the shape of grains became irregular. When a mixture of water and DMSO was used, the tendency to agglomerate was also observed, but the grains retained the spherical shapes and a large distribution of dimensions, with an average diameter of 290±98 nm [14]. The studied surfaces of PEDOT displayed an irregular morphology and evidenced the presence of some grains with mean diameters of 53±32 nm. From an overall morphological perspective, PEDOT·CB7 PRs showed more favorable surface parameters compared to uncomplexed PEDOT, which highlights their potential to generate active layers in organic electronic devices. To understand the factors that control the charge transport within and between PEDOT and the macrocycle CB7, PEDOT·CB7 PSs and PEDOT·CB7 PRs were electrochemically investigated by CV, both samples exhibiting *p*-doping electroactivity. From the onset of oxidation potentials of PEDOT·CB7 PSs and PEDOT·CB7 PRs it was possible to estimate the values of HOMO, whereas the LUMO was estimated from the optical gap. The values of E^{ox}_{onset} were –0.160 V for PEDOT·CB7 PSs and –0.225 V, respectively, for PEDOT·CB7 PRs. Assuming that the HOMO level of ferrocene is –4.80 eV *versus* the vacuum level, the calculated values of the HOMO energy levels were found to be –4.21 and –4.14 eV for PEDOT·CB7 PSs and PEDOT·CB7 PRs, respectively. The LUMO energy levels were calculated from the HOMO energy and the corresponding optical band gaps (ΔE_g^{opt}), leading to values of −2.30 and −2.28 eV for PEDOT·CB7 PSs and PEDOT·CB7 PRs, respectively. HOMO/ LUMO energy levels indicate that the compounds can be applied for device fabrication with compatibility in an organic photovoltaic configuration cell using Al (cathode) and indium tin oxide (ITO) (anode). The measured conductivity, σ_m, of the materials calculated as sum of alternating current conductivity (σ_{AC}) and direct current conductivity (σ_{DC}) indicated that the presence of CB7 improved the conductivity of the PEDOT polymer, due to a higher mobility of the free charges (Fig. 7). Moreover, the conductivity of PEDOT·CB7 PRs was higher compared with that of PEDOT·CB7 PSs and with the reference PEDOT.

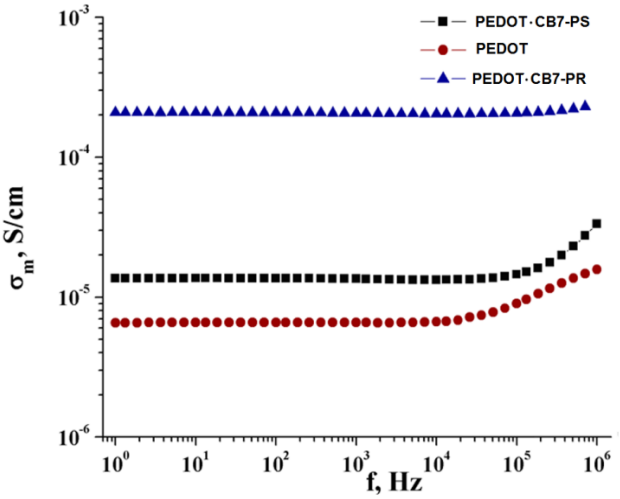

Fig. 7. Evolution of conductivity with frequency for PEDOT·CB7 PS, PEDOT and PEDOT·CB7 PR.

In summary, preparation of these compounds *via* an oxidative polymerization reaction of EDOT·CB7 in water represents a rare case in the literature, in comparison with other EDOT polymerization techniques, and their higher solubility in water or organic solvents should be more promising than the non-rotaxane PEDOT for the generation of active layers in organic electronic devices. In addition, PEDOT·CB7 PSs architectures associated to aerolysin (Ael) nanopore provided evidence for a rapid and real-time probing of the capabilities to form host-guest complexes with various kinds of guest molecules, such as amino acids for protein low-cost sequencing applications [38]. Our attempts at exploring the behaviour of these supramolecular complexes in different electronic devices are currently underway.

4. CONCLUSIONS

This review presents only the most advantageous properties of the selected threaded CPs. These entirely new and original architectures with improved solubility in polar/ nonpolar organic solvents, as well in water, allow their processing by spin coating as thin films, which can be easily integrated as active layers into electronic devices. It is believed that further research in these supramolecular organized systems for organic electronics will continue to deliver excellent achievements in succession to the rapid progress, and there is no doubt that these materials will remain an area of intense and exciting research.

Finally, it should be pointed out that the research in the field started during the doctoral studies of the author under acad. Cristofor I. Simionescu supervision,

almost immediately following the first literature reports (around the year 1994) and continues to be an exciting avenue of research. The impetus for this work is the considerable progress which has been made, and the quality of the research pursued was recognized both internationally and nationally by the scientific community.

Acknowledgements This work was financially supported by the Institute des Études Avancées (IEA) of University of Cergy-Pontoise (Project INEX "Pi-ROT" #73) and the Operational Programme Axis 1– Project "Petru Poni" Institute of Macromolecular Chemistry – Interdisciplinary Pol for Smart Specialization through Research and Innovation and Technology Transfer in Bio(nano)polymeric Materials and (Eco)Technology, InoMatPol (ID P_36_570, Contract 142/10.10.2016, cod MySMIS: 107464).

REFERENCES

1. FACCHETTI A., *π-Conjugated polymers for organic electronics and photovoltaic cell applications*, Chem. Mat., 2011, **23**, 733–758.
2. SHIROTA Y., KAGEYAMA H., *Charge carrier transporting molecular materials and their applications in devices*, Chem. Rev., 2007, **107**, 953–1010.
3. NORIEGA R., RIVNAY J., VANDEWAL K., KOCH F.P.V., STINGELIN N., SMITH P., TONEY M.F., SALLELO A., *A general relationship between disorder, aggregation and charge transport in conjugated polymers*, Nat. Mater., 2013, **12**, 1038–1044.
4. FRAMPTON M.J., ANDERSON H.L., *Insulated molecular wires*, Angew. Chemie Int. Ed., 2007, **46**, 1028–1064.
5. FARCAS A., RESMERITA A.-M., *Supramolecular chemistry: synthesis and photophysical characteristics of conjugated polyrotaxanes*, 2017, Encycl. Phys. Org. Chem., 2017, Wiley, 2543–2582.
6. SFORAZZINI G., KAHNT A., WYKES M., SPRAFKE J.K., BROVELLI S., MONTARNAL D., MEINARDI F., CACIALLI F., BELJONNE D., ALBINSSON B., ANDERSON H.L., *Synthesis and photophysics of coaxial threaded molecular wires: polyrotaxanes with triarylamine jackets*, J. Phys. Chem. C, 2014, **118**, 4553–4566.
7. FARCAS A., AUBERT P.-H., MOHANTY J., LAZAR A.I., CANTIN S., NAU W.M., *Molecular wire formation from poly[2,7-(9,9-dioctylfluorene)-alt-(5,5'-bithiophene/ cucurbit[7]uril)] polyrotaxane copolymer*, Eur. Polym., 2015, **62**, 124–129.
8. FARCAS A., TREGNAGO G., RESMERITA A.-M., TALEB DEHKORDI S., CANTIN S., GOUBARD F., AUBERT P.-H., CACIALLI F., *Effect of permodified β-cyclodextrin on the photophysical properties of poly[2,7-(9,9-dioctylfluorene)-alt-(5,5'-bithiophene)] main chain polyrotaxanes*, J. Polym. Sci., Part A: Polym. Chem., 2014, **52**, 460–471.
9. FARCAS A., JARROUX N., GHOSH I., GUEGAN P., NAU W.M., HARABAGIU V., *Polyrotaxanes of pyrene–triazole conjugated azomethine and α-cyclodextrin with high fluorescence properties*, Macromol. Chem. Phys., 2009, **210**, 1440–1449.
10. FARCAS A., RESMERITA A.-M., AUBERT P.-H., GHOSH I., CANTIN S., NAU W.M., *Synthesis, photophysical, and morphological properties of azomethine-persylilated α-cyclodextrin main-chain polyrotaxane*, Macromol. Chem. Phys., 2015, **216**, 662–670.
11. FARCAS A., LIU Y.-C., NILAM M., BALAN-PORCARASU M., URSU E.-L., NAU W.M., HENNIG A., *Synthesis and photophysical properties of inclusion complexes between conjugated polyazomethines with γ-cyclodextrin and its tris-O-methylated derivative,* Eur. Polym. J., 2019, **113**, 236–243.

12. FARCAS A., ASSAF K.I., RESMERITA A.-M., CANTIN S., BALAN M., AUBERT P.-H., NAU W.M., *Cucurbit[7]uril-based fluorene polyrotaxanes*, Eur. Polym. J., 2016, **83**, 256–264.
13. IDRIS M., BAZZAR M., GUZELTURK B., DEMIR H.V., TUNCEL D., *Cucurbit[7]uril-threaded fluorine-thiophene-based conjugated polyrotaxanes*, RSC Advances, 2016, **6**, 98109–98116.
14. FARCAS A., ASSAF K.I., RESMERITA A.-M., SACARESCU L., ASANDULESA M., AUBERT P.-H.,NAU W.M., *Cucurbit[7]uril-threaded poly(3,4-ethylenedioxythiophene): a novel processable conjugated polyrotaxane*, Eur. J. Org. Chem., 2019, **2019**, 3442–3450.
15. GATHER M.C., BRADLEY D.D.C., *An improved optical method for determining the order parameter in thin oriented molecular films and demonstration of a highly axial dipole moment for the lowest energy π–π* optical transition in poly(9,9-dioctylfluorene-co-bithiophene)*, Adv. Funct. Mater., 2007, **17**, 479–485.
16. FARCAS A., JANIETZ S., HARABAGIU V., GEUGAN P., AUBERT P.H., *Synthesis and electro-optical properties of polyfluorene modified with randomly distributed electron-donor and rotaxane electron-acceptor structural units in the main chain, J.* Polym. Sci. Part A: Polym. Chem., 2013, **51**, 1672–1683.
17. LECLERC M., *Polyfluorenes: twenty years of progress*, J. Polym. Sci. Part A: Polym. Chem., 2001, **39**, 2867–2873.
18. ZHEN C.-G., DAY Y.-F., ZENG W.-J., MA Z., CHEN Z.-K., KIEFFER J., *Achieving highly efficient fluorescent blue organic light-emitting diodes through optimizing molecular structures and device configuration*, Adv. Funct. Mat., 2011, **21**, 699–707.
19. SCHERF U., LIST E.J.W., *Semiconducting polyfluorenes-towards reliable structure-property relationships*, Adv. Mat., 2002, **14**, 477–487.
20. GRIMSDALE A.C., CHAN K.L., MARTIN R.E., JOKISZ P.G., HOLMES A.B., *Synthesis of light-emitting conjugated polymers for applications in electroluminescent devices*, Chem. Rev., 2009, **109**, 897–1091.
21. ZHU Y., GIBBONS M., KULKARNI A.P., JENEKHE A., *Polyfluorenes containing dibenzo[a,c]phenazine segments: synthesis and efficient blue electroluminescence*, Macromolecules, 2007, **40**, 804–813.
22. JUSTINO L.L.G., RAMOS M.L., ABREU P.E., CHARAS A., MORGADO J., SCHERF U., MINAEV B.F., ÅGREN H., BURROWS H.D., *Structural and electronic properties of poly(9,9-dialkylfluorene)-based alternating copolymers in solution: an NMR spectroscopy and density functional theory study*, J. Phys. Chem. C, 2013, **117**, 17969–17982.
23. RICKS A., SOLOMON G., COLVIN M., SCOTT A., CHEN K., RATNER M., WASIELEWSKI M., *Controlling electron transfer in donor–bridge–acceptor molecules using cross-conjugated bridges*, J. Am. Chem. Soc., 2010, **132**, 15427–15434.
24. FARCAS A., JANIETZ S., HARABAGIU V., GUÉGAN P., AUBERT P.-H., *Synthesis and electro-optical properties of polyfluorene modified with randomly distributed electron-donor and rotaxane electron-acceptor structural units in the main-chain*, J. Polym. Sci. Part A: Polym. Chem., 2013, **51**, 1672–1683.
25. FARCAS A., RESMERITA A.-M., AUBERT P.-H., STOICA I., FARCAS F., AIRINEI A., *The effect of permodified cyclodextrins encapsulation on the photophysical properties of a polyfluorene with randomly distributed electron-donor and rotaxane electron-acceptor units*, Beilstein J. Org. Chem., 2014, **10**, 2145–2156.
26. SOZZANI P., COMOTTI A., BRACCO S., SIMONUTTI R., *A family of supramolecular frameworks of polyconjugated molecules hosted in aromatic nanochannels*, Angew. Chem. Int. Ed., 2004, **43**, 2792–2797.
27. FRAMPTON M.J., CLARIDGE T.D.W., LATINI G., BROVELI S., CACIALLI F., ANDERSON H.L., *Amylose-wrapped luminescent conjugated polymers*, Chem. Commun., 2008, **24**, 2797–2799.

28. FARCAS A., JARROUX N., HARABAGIU V., GUÉGAN P., *Synthesis and characterization of a poly [2,7-(9,9-dioctylfluorene-alt-2,7-fluorene/β-CD)] main chain polyrotaxane,* Eur. Polym. J., 2009, **45**, 795–803.
29. FARCAS A., JARROUX N., GUÉGAN P., FIFERE A., PINTEALA M., HARABAGIU V., *Polyfluorene copolymer with a multiply blocked rotaxane architecture in the main chain: synthesis and characterization*, J. Appl. Polym. Sci., 2008, **110**, 2384–2392.
30. FARCAS A., GHOSH I., JARROUX N., HARABAGIU V., GUÉGAN P., NAU W.M., *Morphology and properties of a polyrotaxane based on β-cyclodextrin and a polyfluorene copolymer*, Chem. Phys. Lett., 2008, **465**, 96–101.
31. FARCAS A., TREGNAGO G., RESMERITA A.-M., AUBERT P.-H., CACIALLI F., *Synthesis and photophysical characteristics of polyfluorene polyrotaxanes*, Beilstein J. Org. Chem., 2015, **11**, 2677–2688.
32. FARCAS A., JARROUX N., GUEGAN P., HARABAGIU V., MELNIG V., *Synthesis of a fluorene copolymer with persilylated-cyclodextrin in the main chain*, J. Optoelectron. Adv. M., 2007, **9**, 3484–3488.
33. ZALEWSKI L., BROVELLI S., BONINI M., MATIVETSKY J.M., WYKES M., ORGIU E., BREINER T., KASTLER M., DÖTZ F., MEINARDI F., ANDERSON H.L., BELJONNE D., CACIALLI F., SAMORÌ F., *Self-assembled conjugated thiophene-based rotaxane architectures: structural, computational, and spectroscopic insights into molecular aggregation*, Adv. Funct. Mat., 2011, **21**, 834–844.
34. MICHELS J.J., O'CONNELL M.J., TAYLOR P.N., WILSON J.S., CACIALLI F., ANDERSON H.L., *Synthesis of conjugated polyrotaxanes*, Chem. Eur. J., 2003, **9**, 6167–6176.
35. AL-IBRAHIM M., ROTH H.K., SCHROEDNER M., KONKIN A., ZHOKHAVETS U., GOBSCH G., SCHARFF P., SENSFUSS S., *The influence of the optoelectronic properties of poly(3 alkylthiophenes) on the device parameters in flexible polymer polar cells*, Org. Electron., 2005, **6**, 65–77.
36. KIRCHMEYER S., REUTER K., *Scientific importance, properties and growing applications of poly(3,4-ethylenedioxythiophene)*, J. Mater. Chem., 2005, **15**, 2077–2088.
37. PUTNIN T., LE H., BUI T.-T., JAKMUNEE J., OUNNUNKAD K., PÉRALTA S., AUBERT P.-H., GOUBARD F., FARCAS A., *Poly(3,4-ethylenedioxythiophene/permethylated β-cyclodextrin) polypseudorotaxane and polyrotaxane: synthesis, characterization and application as hole transporting materials in perovskite solar cells*, Eur. Polym. J., 2018, **105**, 250–256.
38. OULDALI H., RESMERITA A.-M., OUKHALED A., FARCAS A., *Exploring interactions of poly(3,4-ethylenedioxythiophene/cucurbit[7]uril) polypseudorotaxane with aerolysin nanopore*, Chem. Commun., CC-COM-09-2019-007135R2.